◆ Human Brain Mapping 36:3104–3116 (2015) ◆

The Trajectory of Disturbed Resting-State Cerebral Function in Parkinson's Disease at Different Hoehn and Yahr Stages

ChunYan Luo,[1] XiaoYan Guo,[1] Wei Song,[1] Qin Chen,[1] Jing Yang,[1] QiYong Gong,[2]* and Hui-Fang Shang[1]*

[1]Department of Neurology, West China Hospital, SiChuan University, Chengdu Sichuan, China
[2]Huaxi MR Research Center, Department of Radiology, West China Hospital, SiChuan University, Chengdu Sichuan, China

Abstract: *Objective:* We aim to investigate the disturbance of neural network associated with the different clinical stages of Parkinson's disease (PD). *Method:* We recruited 80 patients at different H&Y stages of PD (28 at H&Y stage I, 28 at H&Y stage II, 24 at H&Y stage III) and 30 normal controls. All participants underwent resting-state fMRI scans on a 3-T MR system. The amplitude of low-frequency fluctuation (ALFF) of blood oxygen level-dependent signals was used to characterize regional cerebral function. Functional integration across the brain regions was evaluated by a seed voxel correlation approach. *Results:* PD patients had decreased regional activities in left occipital and lingual regions; these regions show decreased functional connection pattern with temporal regions, which is deteriorating as H&Y stage ascending. In addition, PD patients, especially those at stage II, exhibit increased regional activity in the posterior regions of default mode network (DMN), increased anticorrelation between posterior cingulate cortex (PCC) and cortical regions outside DMN, and higher temporal coherence within DMN. Those indicate more highly functioned DMN in PD patients at stage II. *Conclusions:* Our study demonstrated the trajectories of resting-state cerebral function disturbance in PD patients at different H&Y stages. Impairment in functional integration of occipital-temporal cortex might be a promising measurement to evaluate and potentially track functional substrates of disease evolution of PD. *Hum Brain Mapp 36:3104–3116, 2015.*

Key words: Parkinson's disease; Hoehn and Yahr stage; resting-state fMRI; occipital-temporal; default mode network

Additional Supporting Information may be found in the online version of this article.

*Correspondence to: Hui-Fang Shang, Department of Neurology, West China Hospital, Sichuan University, 610041, Chengdu, Sichuan, China. E-mail: hfshang2002@163.com and QiYong Gong, Huaxi MR Research Center (HMRRC), Department of Radiology, West China Hospital of Sichuan University, No. 37 Guo Xue Xiang Chengdu, 610041, China. E-mail: qiyonggong@hmrrc.org.cn

Received for publication 29 January 2015; Revised 8 April 2015; Accepted 24 April 2015.

DOI: 10.1002/hbm.22831
Published online 9 May 2015 in Wiley Online Library (wileyonlinelibrary.com).

INTRODUCTION

Parkinson's disease (PD) is a progressive neurodegenerative disorder that presents with motor symptoms but may also lead to many nonmotor symptoms, such as cognitive impairment and hallucination [Chaudhuri and Schapira, 2009]. The pathological hallmark of PD is the progressive degeneration of dopaminergic neurons in the nigrostriatal pathway. But, the pathologic abnormalities in PD can extend beyond the nigrostriatal pathways and involve other projection neurons of the brainstem and cortex [Braak et al., 2003]. According the staging procedure proposed by Braak [Braak et al., 2003], the spread of pathologic abnormalities following an ascending pattern from lower brainstem to cortical areas.

During the past decade, in vivo imaging of the brain structural changes has offered powerful measurements of assessing neurodegenerative changes in PD. High resolution MRI can accurately measure changes in cerebral structures. While previous studies showed no or only slight frontal and temporal [Borghammer et al., 2010; Burton et al., 2004; Melzer et al., 2012; Nagano-Saito et al., 2005; Nishio et al., 2010; Weintraub et al., 2011] gray matter (GM) loss in early to mild nondemented PD patients, there is a marked GM atrophy of the limbic, temporal, frontal, and parietal regions in PD patents at advanced stage or demented PD patients [Burton et al., 2004; Melzer et al., 2012; Weintraub et al., 2011]. More recent studies have also shown that cortical thinning occurs in PD [Jubault et al., 2011; Lyoo et al., 2010]. Through modeling disease stage, Zarei [Zarei et al., 2013] further found that disease stage in PD was associated with thinning of the medial frontal, precuneus, lateral occipital, temporal, and dorsolateral prefrontal cortex. In addition, white matter (WM) loss has been detected in early to moderate stages of the disease, in the pons, as well as in temporal and frontal regions [Jubault et al., 2009; Kostic et al., 2010]. By diffusion tensor imaging (DTI), abnormalities of WM integrity have been identified in demented PD patients [Hattori et al., 2012]; and evidence of degeneration in WM has also been revealed in PD patients without dementia [Hattori et al., 2012; Karagulle Kendi et al., 2008]. Generally, microstructural damage to the WM occurs with increasing PD severity and involves the brainstem, thalamocortical pathways, olfactory tracts, as well as the major interhemispheric, limbic, and extramotor association tracts [Agosta et al., 2013].

Studies using advanced methods of time series analysis of oscillatory brain activity have demonstrated that synchronization of neuronal activity within and between distributed neuronal populations is an important mechanism in a variety of cognitive and motor functions, including movement preparation, sensorimotor integration and attention [Schnitzler and Gross, 2005]. Previous studies have suggested PD is characterized by changing patterns of disturbed neural synchrony that appear to be dependent on the stage of disease [Berendse and Stam, 2007]. Resting-state fMRI (rfMRI) allows the interrogation in vivo of the neural synchrony disturbance. It can provide information not only on synchronous regional cerebral activity using the amplitude of low-frequency fluctuation (ALFF) intensity, but also on the integrity of brain networks using connectivity analysis. This technique has been successfully utilized to detect abnormal functional integration in PD [Esposito et al., 2013; Luo et al., 2014; Tessitore et al., 2012]. However, few experiments have used this technique in an effort to depict the changing course of abnormal functional integration in PD. It remains unclear how disturbances of functional brain networks evolve throughout the course of the disease.

The aim of this study was to investigate the functional changes of neural network associated with the different clinical stages of PD, thus reveal the possibly different trajectories of functional damage in PD. To approach this issue, we used rfMRI in a relatively large cohort of PD patients at different Hoehn and Yahr (H&Y) stages (I–III). We believe that our study would allow us to improve our understanding of PD pathobiology and contribute to the identification of new markers for monitoring its evolution in vivo.

METHODS

Participant

The local research ethics committee approved this study, and written informed consent was obtained from all participants. The patients in the present analysis were part of a large cohort study of PD in the Chinese population of Han ethnic background. Patients with right dominant hand were recruited consecutively from Movement Disorders outpatient clinic of West China Hospital of Sichuan University. All patients fulfilled the PD Society Brain Bank diagnostic criteria and were followed at least two years to confirm the diagnoses. All patients were clinically stable. To date, no indication of atypical parkinsonism has been detected in any of our PD patients according to the clinical diagnostic criteria for parkinsonism disorders appraised by the Movement Disorders Society Task Force. From this cohort, patients were excluded if they had (1) moderate-severe head tremor; (2) abnormal MMSE (mini-mental state examination) scores; (3) cerebrovascular disorders including previous stroke, history of head injury, history of seizure, hydrocephalus, or intracranial mass, previous neurological surgeries; (4) had any disorder that interfered with the assessment of the manifestation of PD. On the basis of previous studies using MMSE in Chinese [Katzman et al., 1988; Zhang et al., 1990], we used the following cutoff points to define abnormal MMSE in our patients: 17 for illiterate subjects, 20 for grade-school literate, and 24 for junior high school and higher education literate. A total of 80 patients were recruited: 28 PD patients at Hoehn and Yahr (H&Y) stage I, 28 PD patients at H&Y stage II and 24 PD patients at H&Y stage III.

The experiments were performed at least 12 h after the last dose of dopaminergic medication (i.e., in a practically

TABLE I. Clinical features of subjects

	Patients with PD			
	H&Y Stage I	H&Y Stage II	H&Y Stage III	Controls
N	28	28	24	30
Gender (male:female)	14:14	14:14	13:11	15:15
Age (years)	52.45 ± 9.18	54.12 ± 8.24	54.41 ± 10.59	53.53 ± 10.45
Side of onset (R:L)	15:13	13:15	11:13	–
Duration (years)	1.56 ± 1.42	3.78 ± 2.87	5.31 ± 4.77	–
UPDRS III score	14.11 ± 6.45	29.68 ± 8.22	43.54 ± 12.65	–
MMSE score	28.29 ± 2.12	27.89 ± 1.93	26.25 ± 2.75	–

defined off-condition) [Helmich et al., 2010]. Data pertaining to age, gender, handedness, duration of illness, and clinical symptom ratings were collected by movement disorder specialist prior the initiation any treatment and magnetic resonance (MR) examinations. Disease duration was defined as the time as the patient subjectively noticed his first motor symptoms. Unified PD Rating Scale (UPDRS) part III was used to assess motor disability and H&Y stages was used to evaluate the severity of the disease.

Additionally, 30 right-handed normal subjects with no history of neurologic or psychiatric diseases were recruited from friends and spouses of the patients and matched for age, gender with the PD subjects.

MRI Acquisition

MRI was performed on a 3.0 Tesla MR imaging System (Excite; GE, Milwaukee, WI) using an eight-channel phased-array head coil. MR images sensitized to changes in BOLD signal levels (TR = 2000 ms, echo time = 30 ms, flip angle = 90°) were obtained via a gradient-echo echo-planar imaging sequence (EPI). The slice thickness was 5 mm (no slice gap) with a matrix size of 64 × 64 and a field of view of 240 × 240 mm^2, resulting in a voxel size of 3.75 × 3.75 × 5 mm^3. Each brain volume comprised 30 axial slices and each functional run contained 200 image volumes. The fMRI scanning was performed in darkness, and the participants were explicitly instructed to relax, close their eyes and not fall asleep (confirmed by subjects immediately after the experiment) during the resting-state MR acquisition. Earplugs were used to reduce scanner noise, and head motion was minimized by stabilizing the head with cushions.

Processing of fMRI Data

Image preprocessing and statistical analysis were carried out using the SPM8 (Welcome Department of Imaging Neuroscience, London, UK; http://www.fil.ion.ucl.ac.uk). The first ten volumes of functional images were discarded for the signal equilibrium and participants' adaptation to scanning noise. Then, the remaining EPI images were preprocessed using the following steps: slice timing, motion correction, spatial normalization to the standard Montreal Neurological Institute (MNI) EPI template in SPM8 and resample to 3 × 3 × 3 mm^3, followed by spatial smoothing with 8-mm full-width at half-maximum (FWHM) Gaussian kernel. According to the record of head motions within each fMRI run, all participants had less than 1.5 mm maximum displacement in the *x*, *y*, or *z* plane and less than 1.5° of angular rotation about each axis.

Local Function Investigation

ALFF Calculation

Given the importance of low-frequency fluctuations in determining resting-state activity, the analysis of low-frequency signal power has emerged as a fruitful approach to characterizing the local health of resting-state networks. ALFF maps were calculated using REST (http://restfmri.net/forum/rest_v17). After preprocessing, the time series for each voxel was filtered (band pass, 0.01–0.08 Hz) and linear-trend removed. Then, the filtered time series was transformed to a frequency domain using a fast Fourier transform, and the power spectrum was square root-transformed and averaged across the frequency of 0.01–0.08 Hz at each voxel. This averaged square root of activity was taken as the ALFF. For standardization purposes, the ALFF of each voxel was divided by the global mean ALFF value to standardize data across subjects.

Voxel-based comparison of ALFF maps among the four groups was performed using a design model of one-way analysis of variance with age and gender as covariates. The significance threshold of f test was set at $P < 0.001$ and cluster size >50 voxels. Mean value was extracted in each region showing significant difference by averaging the ALFF value within seed region. Post hoc two sample *t*-tests were performed.

Functional Connectivity Analysis

Functional connectivity was examined using a seed voxel correlation approach. As shown below, significant

difference in ALFF measurements among four groups was demonstrated in 4 brain regions (Table I). These 4 regions were used as seeds for functional connectivity analysis. After bandpass filtering (0.01–0.08 Hz) [Cordes et al., 2001] and linear trend removal, the reference time series for each seed region was extracted by averaging the fMRI time series of all voxels within each of the 4 regions. Correlation functional analyses were performed by computing temporal correlation between each seed reference and the rest of the brain in a voxel-wise manner. To remove the possible variances from time course of each voxel, eight nuisance covariates were regressed, including: the white matter (WM) signal, the CSF signal and six head motion parameters obtained in the realigning step. Then, the correlation coefficients in each voxel were transformed to z-value images using the Fisher r-to-z transformation to improve normality [Lowe et al., 1998]. Therefore, an entire brain z-value map was created for each subject.

Voxel-based comparison of z-value maps among the four groups was also performed, using a design model of one-way analysis of variance with age and gender as covariates. The significance threshold of f test was set at $P < 0.001$ and cluster size >50 voxels. Mean value was extracted in each region showing significant difference by averaging the z value within seed region. Post hoc two sample t-tests were performed.

TABLE II. Regions showing significant difference in ALFF value among PD subgroups and controls

Anatomic region	Coordinates of peak voxel (x y z)[a]	Peak F	Cluster size
Precunes/PCC	−3 −45 33	9.45	190
Right Lateral Parietal	45 −51 45	10.51	149
Left Inferior Occipital	−18 −93 −9	10.92	210
Left Lingual	−18 −57 −6	8.79	102

[a]x, y, and z are location of peak voxel in the MNI coordinate.

Correlation Analysis

To assess whether the UPDRS III/MMSE scores were associated with changes in regional function and related network, UPDRS III/MMSE scores and ALFF/z-value maps were entered into the corresponding design matrix using linear regression model with age and gender as covariates. In voxel-wise regression analysis, clusters with voxel level $P < 0.001$ and size >50 voxels were reported.

Region-Wise Functional Connectivity in Default Mode Network

To evaluate functional connectivity within default mode network (DMN), 13 regions derived from Fox et al. [2005] were selected as graph network nodes (Supporting Information Table S2), and then a correlation between each pair was analyzed. Mean time series were extracted by averaging the time series of each peak voxel and its nearest 26 neighbors. The resting-state BOLD time series were correlated region by region for each subject. For each subject, then, we created a square (13 × 13) correlation matrix, resulting in 110 matrices. Fischer z transformation was applied to the correlation coefficients (r) to improve normality for the random effects analysis. To further localize specific pairs of brain regions in which functional connectivity was altered, we used a network-based statistic (NBS) approach [Zalesky et al., 2010]. One-way ANOVA analysis was preformed on all potential connection represented in the 13 × 13 correlation matrices. In brief, a primary cluster-defining threshold ($F = 2.7$, $P = 0.05$) was first used to identify suprathreshold connections, within which the size (i.e., number of edges) of any connected components was then determined. A corrected P value was calculated for each component using the null distribution of maximal connected component size, which was derived empirically using a nonparametric permutation approach (5000 permutations). Of note, the effects of age and gender were removed by a regression analysis prior to the statistical analysis of functional connections.

Processing of Structural Images

Voxel-based morphometry (VBM) analysis was performed for structural images. In this study, we used the diffeomorphic anatomic registration through an exponentiated lie algebra algorithm (DARTEL) [Ashburner, 2007] to improve the registration of the MRI images. DARTEL has been shown to be more sensitive than standard VBM methods [Klein et al., 2009]. Before segmentation, we checked for scanner artifacts and gross anatomical abnormalities for each subject; and the image origin was set to the anterior commissure. Then, MR images were segmented into gray matter (GM), WM and CSF using the unified segmentation model in SPM8 [Ashburner and Friston, 2005]. In a next step, a GM template was generated through an iteratively nonlinear registration (DARTEL). The GM template was normalized to MNI space and the resulting deformations were applied to the GM images of each participant. Finally, spatially normalized images were modulated to ensure that the overall amount of each tissue class was not altered by the spatial normalization procedure, and smoothed with an 8-mm FWHM Gaussian kernel. Voxel-based comparison of GM volume among the four groups was performed using a design model of one-way analysis of variance with age and gender as covariates. The significance threshold of f test was set at $P < 0.001$. Cluster with number of voxels >200 were reported. Mean value was extracted in each region showing significant difference by averaging the value within seed region. Post hoc two sample t-tests were performed.

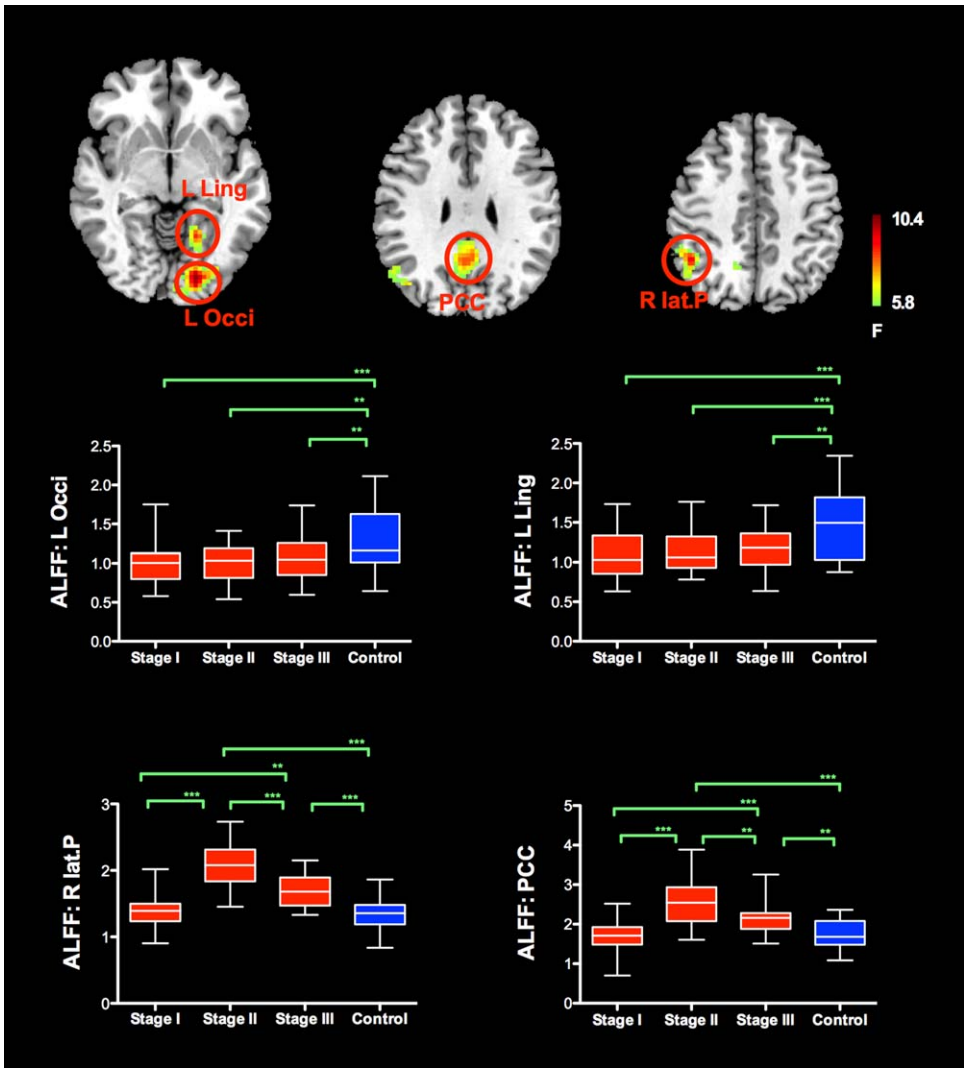

Figure 1.

The group level ALFF analysis revealed significant group differences in PCC/precuneus, right lateral parietal cortex, left occipital cortex and left lingual gyrus. Compared with normal control subjects, PD patients showed significant decreased ALFF in the left occipital cortex and left lingual gyrus in comparison to normal controls. Conversely, PD patients at H&Y stage II and III showed higher ALFF in the posterior cingulate cortex and right lateral parietal cortex. The pattern of increased ALFF in PD patients across different H&Y stages (I-III) was more prominent in patients at H&Y stage II and resembles inverted "V" type. Abbreviation L: left; R: right; Occi: occipital; Ling: lingual; lat.P: lateral parietal; PCC: posterior cingulate cortex. [Color figure can be viewed in the online issue, which is available at wileyonlinelibrary.com.]

RESULTS

Clinical Characteristics of the PD Groups

Demographic and clinical features of the sample were listed in Table I. Age, gender and side of onset were not significantly different among four subgroups. By definition, there was significant difference in disease duration and UPDRS motor score among PD subgroups. Though PD patients were free from overt cognitive impairment, patients at stage III gain significantly lower MMSE score than other patients ($P < 0.05$).

Regional Cerebral Function

Figure 1 and Table II show the group level results of ALFF analysis. There were significant group differences in posterior cingulate cortex/precuneus (PCC), right lateral parietal cortex, left occipital cortex and left lingual gyrus.

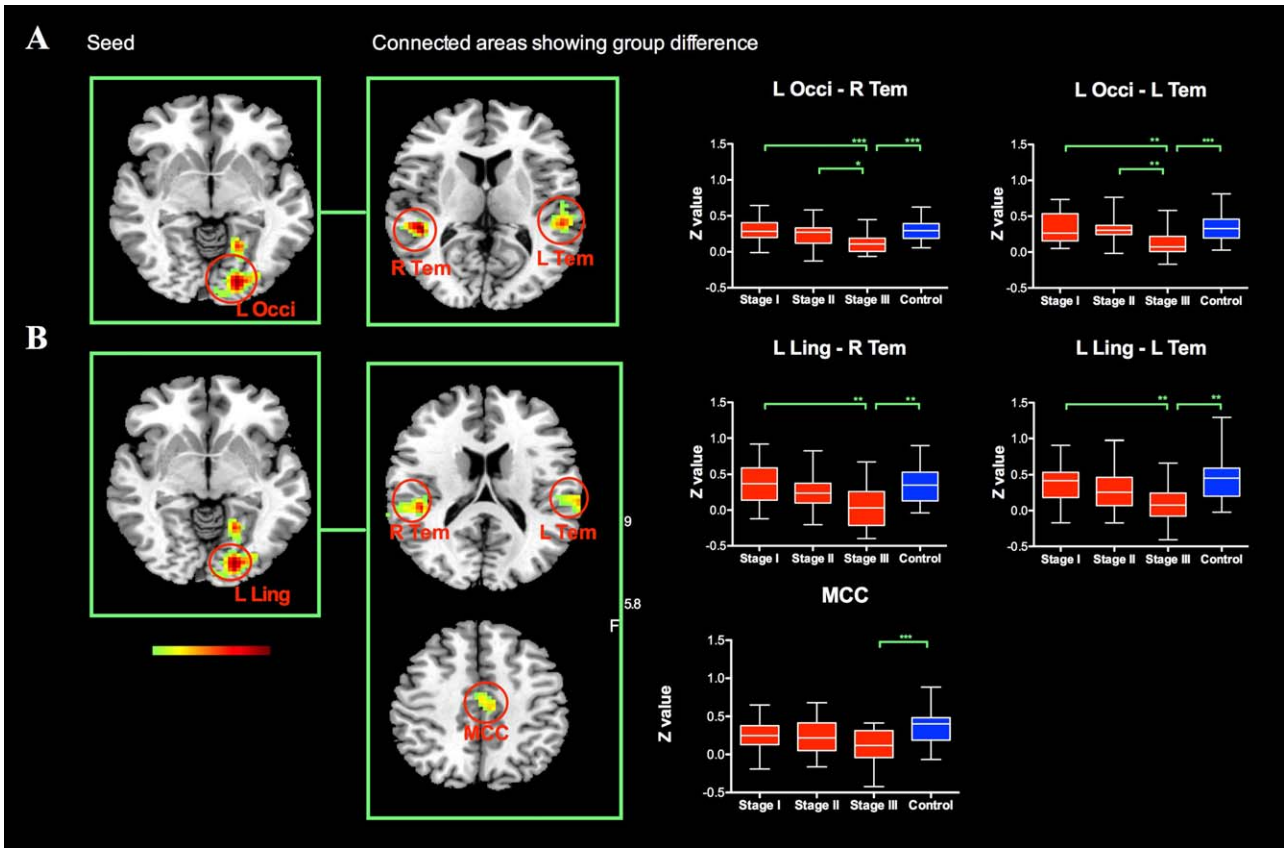

Figure 2.

The group level analysis of the FC maps of left occipital cortex and left lingual gyrus revealed significant group differences in bilateral temporal cortex. PD patients at H&Y stage III demonstrated significant decreased functional connectivity of left occipital cortex/left lingual gyrus with bilateral temporal cortex. In PD patients, the functional connectivity of left occipital–temporal circuit showed descending pattern as H&Y stage ascending. Abbreviation: L: left; R: right; Occi: occipital; Ling: lingual; Tem: temporal; MCC: middle cingulate cortex. [Color figure can be viewed in the online issue, which is available at wileyonlinelibrary.com.]

Two sample *t*-tests revealed compared with control subjects, PD patients at stage II and III showed higher ALFF in the posterior cingulate cortex and right lateral parietal cortex. The pattern of increased ALFF was more prominent in patients at stage II. Conversely, all PD patients showed significant decreased ALFF in the left occipital cortex and left lingual gyrus in comparison to normal controls. Those regions showing group difference were then selected as seed regions for connectivity analysis.

Seed-Based Functional Connectivity Analysis

Analysis of the FC maps of left occipital cortex and left lingual gyrus revealed significant group differences in bilateral temporal cortex (Fig. 2 and Table III). Post hoc analysis revealed that, compared to controls, PD patients at stage III demonstrated significant decreased functional connectivity of left occipital cortex/left lingual gyrus with bilateral temporal cortex. In PD patients, the functional connectivity of left occipital–temporal circuit showed descending pattern as H&Y stage ascending.

Analysis of the FC maps of PCC revealed group differences in supplementary motor area, bilateral insular, bilateral sensorimotor area, bilateral inferior parietal cortex, and retrosplenial cortex (Fig. 3). In comparison to control group, the functional connectivity of PCC with supplementary motor cortex, bilateral insular, bilateral sensorimotor cortex and bilateral inferior parietal cortex were relatively decreased in PD patients, and further shift to negative connectivity pattern. This anti-correlation pattern (negative functional connectivity of PCC) was most prominent in PD patients at stage II. Conversely, PCC shows positive correlation with retrosplenial cortex. The

TABLE III. Difference of functional connections to left occipital, lingual and PCC among PD subgroups and controls

Connected location	Coordinates of peak voxel (*x*, *y*, *z*)[a]	Peak F	Cluster size
Seed Area: Left Occipital			
Right temporal	45 −39 6	10.39	143
Left temporal	−51 −33 6	9.56	116
Seed area: Left lingual			
Right temporal	45 −33 18	8.62	120
Left temporal	−42 −12 12	7.47	125
Right temporal	54 −15 3	8.56	94
Left temporal	−54 3 −9	8.86	63
Left middle cingulate	−9 −15 48	7.26	88
Seed Area: PCC			
Supplementary motor area	0 −3 60	10.97	342
Retrosplenial	−3 −54 12	9.31	143
Left postcentral	−42 −9 18	7.86	117
Left insula	−51 12 −3	8.3	112
Right inferior parietal	33 −48 48	8.36	70
Left inferior parietal	−30 −42 42	8.42	54
Right precentral	48 −6 45	8.37	59
Right insula	48 12 0	8.63	64

[a] *x*, *y*, and *z* are location of peak voxel in the MNI coordinate.

functional connectivity of PCC with retrosplenial cortex was significantly increased in PD patient at stage II compared with normal controls. The functional connectivity analysis seeding at left lateral parietal cortex did not yield any significant difference between any of four groups.

Correlation Analysis

In PD patients, the UPDRS III score was negatively correlated with the *z* values of the left lingual/occipital regions with bilateral temporal regions (Fig. 4). MMSE score was positively correlated with *z* values of left lingual/occipital regions with occipital regions.

Region-Wise Functional Connectivity in DMN

As described above, PD patients at H&Y I-III display increased regional spontaneous activity in PCC/Precuneus and lateral parietal cortex. PCC/Precuneus has been suggested to be the "core node" of the default mode network (DMN) that is activated during "resting consciousness." Lateral parietal cortex is also recognized as an important region of DMN. Analysis was conducted to characterize the functional integrity within DMN. The mean correlation matrix was calculated by averaging the correlation matrix across all subjects within each group. For better visualization of structural patterns within those connection matrices, a layout of nodes and undirected edges were represented as networks (Fig. 5). According to Figure 5A, functional connectivity appeared to be dense in PD patients, particularly in patients at stage II. To directly compare connectivity (r) of each pair node between the two groups, one-way ANOVA were performed on all 78 potential connections included in the correlation matrices. We utilized the NBS method to identify a single connected network with 11 nodes and 17 connections, which was significantly different among groups ($P = 0.036$, corrected) (Fig. 5B, Supporting Information Table S3). Within this network, 15 connections exhibited increased values in the PD patients, especially in PD patients at stage II, compared with the control subjects (Fig. 5C). Two connections showed relatively decreased values in PD patients as compared with the controls. Together with the above results of PCC showing increased functional connectivity with retrosplenial cortex in PD patient at stage II, those results indicate that the default network and associated regions are highly integrated (i.e., strongly functionally connected) in PD patients at stage II.

Structural Assessment

VBM analysis revealed that one cluster in right thalamus shows group difference of GM volume. Post hoc analysis indicated PD patients at early stage (especially those at H&Y I) have relatively higher GM volume than controls in this region (Fig. 6). There was no significant cortical atrophy in PD patients.

DISCUSSION

To date, very few studies have focused on mapping out the trajectory of functional neural changes of PD patients. In this study, we applied rfMRI measures on a relatively large cohort of PD patients across different H&Y stages (I–III). We found that: (a) PD patients had deceased regional activities in left occipital and lingual regions; these regions show decreased functional connection pattern with temporal regions, which is deterring as H&Y stage ascending and negatively correlated with UPDRS III score; (b) PD patients, especially those at stage II, exhibit increased regional activity in the posterior regions of DMN, increased anticorrelation—that is, more negatively connection between PCC and some cortical regions outside DMN, and higher temporal coherence within DMN, which indicate more highly functioned DMN in PD patients at stage II.

Reduction of either activation, perfusion, or metabolism in occipital and temporal regions during rest or simple visual stimulation has been frequently observed in PD patients with or without dementia [Abe et al., 2003; Baglio et al., 2011; Bohnen et al., 1999; Eberling et al., 1994; Hu et al., 2000; Peppard et al., 1992; Schwartzman et al., 1988]. Additionally, emerging neuroanatomy studies reported GM loss in occipital–temporal association areas[Lyoo et al., 2010; Melzer et al., 2012; Weintraub et al., 2011].

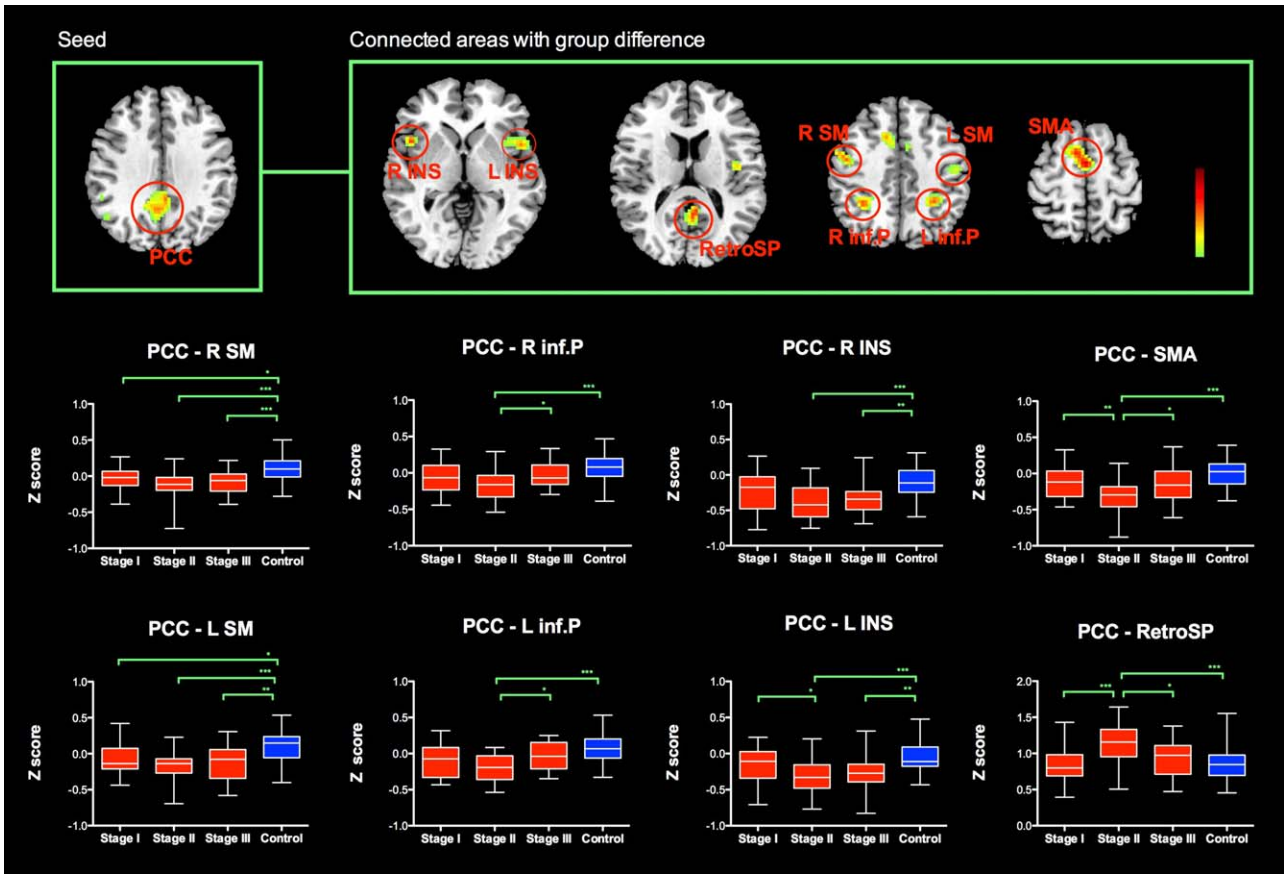

Figure 3.

The group level analysis of the FC maps of PCC revealed group differences in supplementary motor area, bilateral insular, bilateral sensorimotor area, bilateral inferior parietal cortex and retrosplenial cortex. In comparison to control group, the functional connectivity of PCC with supplementary motor cortex, bilateral insular, bilateral sensorimotor cortex and bilateral inferior parietal cortex were relatively decreased in PD patients, and further shift to negative connectivity pattern. The anticorrelation pattern (negative functional connectivity of PCC) was most prominent in PD patients at H&Ystage II. Conversely, PCC shows positive correlation with retrosplenial cortex. The functional connectivity of PCC with retrosplenial cortex was significantly increased in PD patient at H&Y stage II compared with normal controls. Abbreviation: L: left; R: right; PCC: posterior cingulate cortex; SM: sensorimotor area; inf.P: inferior parietal cortex; INS: insular; SMA: supplementary motor area; RetroSP: retrosplenial cortex. [Color figure can be viewed in the online issue, which is available at wileyonlinelibrary.com.]

Using rfMRI measurements, decreased ALFF value [Zhang et al., 2013] and loss of functional connectivity in occipital regions (mostly involving temporal brain regions) [Olde Dubbelink et al., 2014] in patients with PD have been observed. Our study is consistent with those previous studies, and reaffirming the involvement of the occipital–temporal cortex in PD patients at early to moderate stages. Together with previous results, it seems appropriate to conclude that occipital–temporal dysfunction is a significant feature of PD. Cortical regions at occipital–temporal regions are involved in processing the visual information [Downing et al., 2006; Grill-Spector, 2003; Malach et al., 1995]. According to former researches, hypofunction of occipital–temporal regions is responsible for aberrant cortical visual processing in PD [Abe et al., 2003; Ishioka et al., 2011]. And, impaired object perception has been described in PD patients[Barnes et al., 2003; Laatu et al., 2004; Pieri et al., 2000; Price et al., 1992; Uc et al., 2005], even at a mild stage of the disease[Pieri et al., 2000; Price et al., 1992]. Besides, cognitive impairment in PD has also been associated with marked hypoperfusion or hypometabolism in visual association cortices [Bohnen et al., 2011]. Thus, the reduced baseline activity in the occipital lobe and impaired functional integration of occipital–temporal regions in our study are likely to be related to these clinical background factors, and indicate a preclinical dysfunction of the visual information processing, which is associated with cognitive impairment in PD.

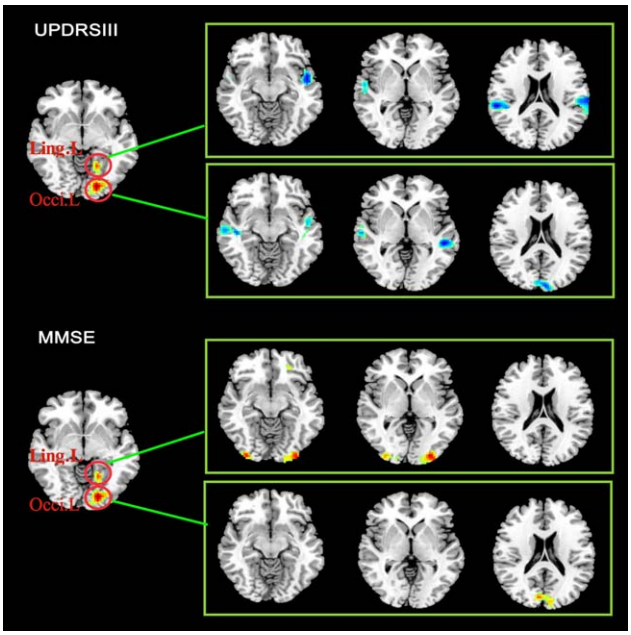

Figure 4.

UPDRS III score was negatively correlated with the z values of the left lingual/occipital regions with bilateral temporal regions in PD patients. MMSE score was positively correlated with z values of left lingual/occipital regions with occipital regions. Abbreviation: L: left; R: right; Occi: occipital; Ling: lingual. [Color figure can be viewed in the online issue, which is available at wileyonlinelibrary.com.]

Moreover, our study shows that the functional integrity of occipital–temporal circuits decreased in PD patients as H&Y stage ascending. More impairment of occipital–temporal regions has been reported in PD patients at advanced stage relative to patients at mild stage [Melzer et al., 2012; Nagamachi et al., 2008; Weintraub et al., 2011]. In addition, continuous decrease in functional connectivity of occipital and temporal regions over time has been observed in the above-mentioned study [Olde Dubbelink et al., 2014]. In accordance with those finding, our results of decreased functional integrity of occipital–temporal circuits might also reflect the severity of the pathological condition of PD. This deteriorating pattern of functional integrity of occipital–temporal circuits could account for visuo-perceptual and cognitive deficits that arise as the disease evolves. In the supplementary analysis (see Supporting Information), we found the visuospatial subscore of Addenbrooke's Cognitive Examination-Revised (ACE-R) was positively correlated with the functional connectivity of occipital-temporal network in another cohort, giving support to our hypothesis. However, in the present study, we did not find significant correlation between functional integrity in occipital–temporal circuits and MMSE score. The lack of correlation in our study is likely due to 1) our patients were without apparent cognitive impairment; 2) MMSE score is not sensitive to subtle cognitive changes or impairment in one particular cognitive subdomain. Instead, we found functional integrity in occipital–temporal circuits is negatively correlated with UPDRS score. The reduced functional integrity in occipital–temporal circuits revealed by our study might result in impaired processing of external visual information and/or deficient information transformation from the "down" processing regions to the "up" regions for further processing, and thus could contribute to motor impairment through deficit sensorimotor integration. Or, this relationship could reflect the parallel deterioration of motor impairment and impaired visuoperceptual processing in PD patients caused by disease evolution. Nevertheless, impaired integration in occipital–temporal cortex might be a new potential marker for monitoring disease evolution in PD.

Contrary to decreased regional activity and functional integration in visual association regions, our study found PD patients, especially those at stage II, display increased regional activity in the posterior regions of DMN and higher temporal coherence within DMN. The DMN is a set of brain regions that have been observed to consistently active in rest and deactivated during active task states [Raichle et al., 2001], and referred as self-referential activity [Broyd et al., 2009; Gusnard et al., 2001]. Our results are likely to indicate enhanced intrinsic, self-referential process in PD patients at stage II. Attenuated external information input has been suggested to result in an increase of internally generated activity [Vanhaudenhuyse et al., 2011]. We postulate that the enhanced function of intrinsic network observed in our study could also result from attenuated external information input to extrinsic network, which come along with progressive motor dysfunction or pathological changes in visual processing system.

Recent studies have detected a network termed the task-positive network (TPN) that functions as a counterpart of the DMN in the form of anticorrelation between spontaneous activities occurring in the two networks [Fox et al., 2005]. This network comprise mainly inferior parietal lobule, precentral sulcus, supplementary motor area, dorsal lateral prefrontal cortex and insular, which play important role in motor control. In the current study, the results that PCC negatively predicted activity in those regions in PD patients are in line with previous studies showing the competing character of the two systems (intrinsic and extrinsic brain networks) [Fransson, 2005]. Additionally, PD patients, especially those at H&Y stage II, were characterized by a more widespread, temporally dynamic interaction between PCC and TPN regions. Anticorrelation has great significance in states of higher vigilance [Chang et al., 2013; Horovitz et al., 2009; Samann et al., 2011] and inhibitory control performance[Barber et al., 2013]. But, it would be counterproductive when the interaction between these two networks is unbalanced. In normal state, anticorrelation could enhance the coordination of its

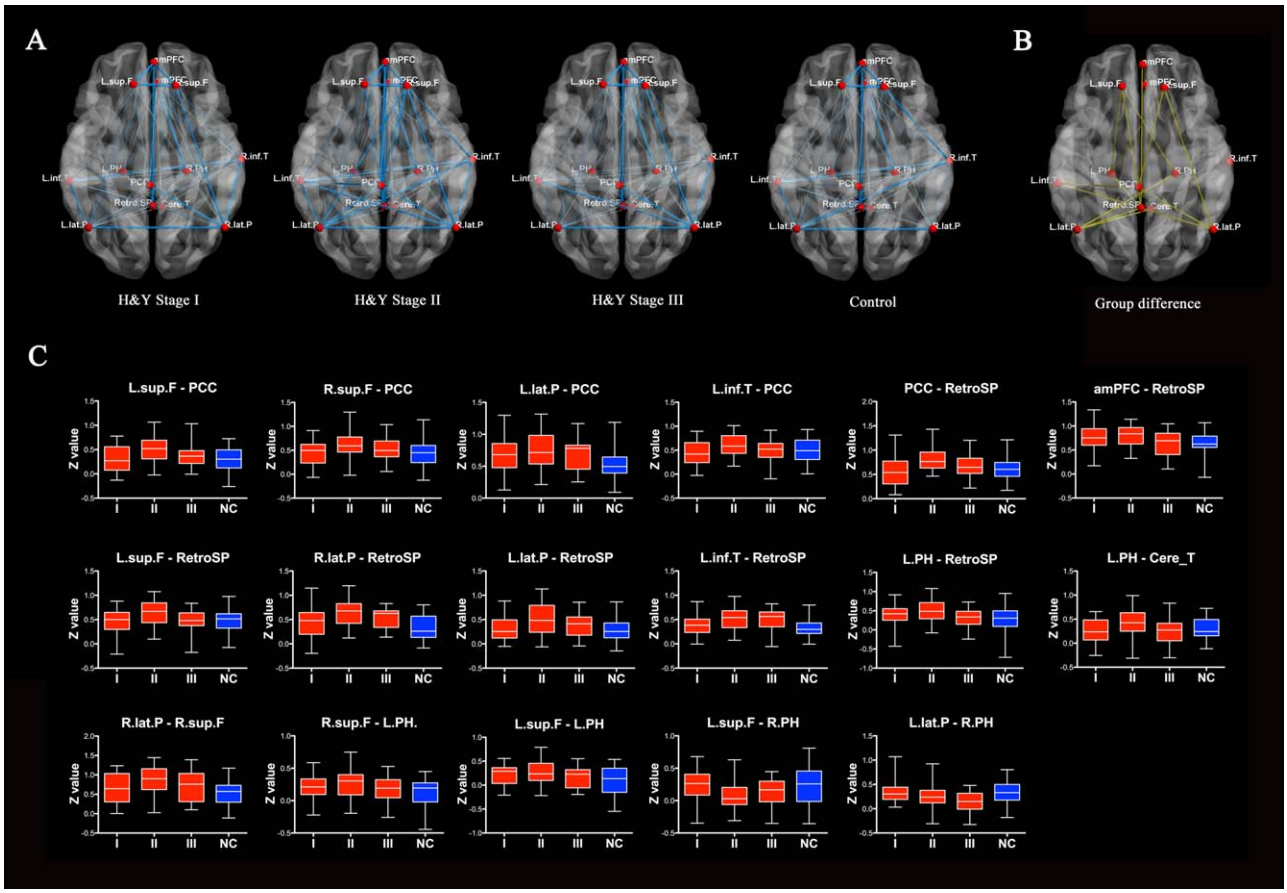

Figure 5.

(**A**) Graph visualization of the mean connectivity within DMN in controls and PD patients across different H&Y stage (I–III). Undirected edges (functional connectivity) are demonstrated with two different width lines according to three different connection strengths ($r > 0.2$ and $r > 0.4$). (**B**) Graph represents the differences in region-wise functional connectivity among the four groups ($P = 0.036$, corrected). (**C**) Among those connections, 15 connections exhibited increased values in the PD patients, especially in PD patients at stage II, as compared with the controls. Two connections showed relatively decreased values in PD patients as compared with the controls. Abbreviation: see Supporting Information Table S2. [Color figure can be viewed in the online issue, which is available at wileyonlinelibrary.com.]

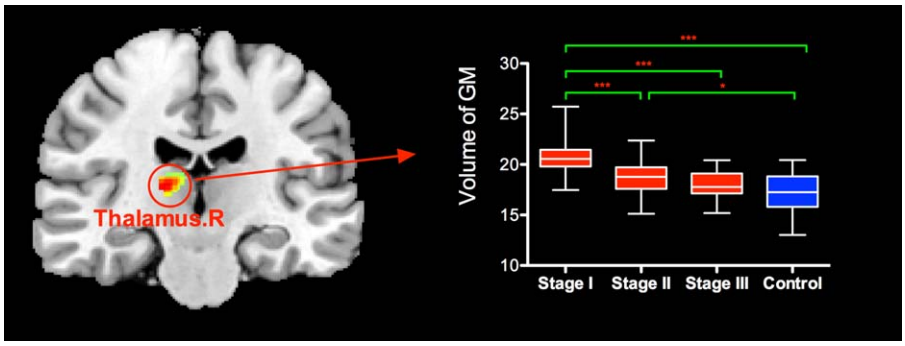

Figure 6.

VBM analysis revealed PD patients at early stage (especially those at H&Y stage I) have relatively higher gray matter (GM) volume than controls in right thalamus. [Color figure can be viewed in the online issue, which is available at wileyonlinelibrary.com.]

antinetworks. However, as highly functioned DMN emerged, the balance was broken, with abnormally greater influence of default mode regions on TPN regions. Our results could represent this imbalanced state of interaction between DMN and TPN in PD patients at H&Y stage II.

Contradictory results regarding the DMN integrity in PD have been reported in the available studies. The earlier studies did not find any difference between the nondemented PD and HC groups in the DMN[Krajcovicova et al., 2012; Rektorova et al., 2012]. Then, decreased functional connectivity of DMN in the right medial temporal lobe and bilateral inferior parietal cortex were reported in a resting-state fMRI study that evaluated cognitively unimpaired PD patients [Tessitore et al., 2012]. However, using a similar data-driven method, a recent study reveal no significant connectivity differences were observed between HC and cognitive unimpaired PD for DMN, but significant increased connectivity of DMN in posterior cortical regions in PD patients with cognitive impairment [Baggio et al., 2014]. Instead of a plain ascending or descending pattern, the observed difference related to DMN in our study was most prominent in the PD patients at stage II, which resembles"V"or inverted "V" type. This observation might underline the inconsistent results reported in the available studies. We proposed that, at relatively early stage, reduction in afferent information could contribute to imbalance between intrinsic and extrinsic system, thus result in highly functioned intrinsic system-DMN. However, as the disease progress, more cortical regions were involved by the spread of pathologic abnormalities, including those regions constitute the DMN. Thus, those DMN regions cannot sustain the relatively high level of functions. Nevertheless, more studies are needed to elucidate the dynamic change of DMN function and its clinical relevance in PD patients.

Some limitations of our study need to be addressed. First, though we study disease evolution by comparing PD at different stages, we recognize that this cross-sectional design does not replace a well-designed longitudinal study. Further longitudinal studies are required to confirm our findings. In addition, to avoid the confounding factors of comparing groups with a different aging-related pathology, we enrolled patients with similar age, but with different degrees of functional worsening. This approach could also raise other confounding factors; for instance, the age at onset of the disease was different between groups.

In conclusion, our study reveal the trajectories of resting-state cerebral function disturbance in PD patients at different H&Y stages, and provide vital information that might contribute to the understanding of the pathological mechanisms associated with the progression of PD. Though further investigation is required, our findings suggest that impairment in functional integration of occipital–temporal cortex might be a promising measurement to evaluate and potentially track functional substrates of disease evolution of PD.

REFERENCES

Abe Y, Kachi T, Kato T, Arahata Y, Yamada T, Washimi Y, Iwai K, Ito K, Yanagisawa N, Sobue G (2003): Occipital hypoperfusion in parkinson's disease without dementia: Correlation to impaired cortical visual processing. J Neurol Neurosurg Psychiatry 74:419–422.

Agosta F, Canu E, Stojkovic T, Pievani M, Tomic A, Sarro L, Dragasevic N, Copetti M, Comi G, Kostic VS , Filippi M. (2013): The topography of brain damage at different stages of parkinson's disease. Hum Brain Mapp 34:2798–2807.

Ashburner J. (2007): A fast diffeomorphic image registration algorithm. Neuroimage 38:95–113.

Baggio HC, Segura B, Sala-Llonch R, Marti MJ, Valldeoriola F, Compta Y, Tolosa E, Junque C. (2014): Cognitive impairment and resting-state network connectivity in Parkinson's disease. Hum Brain Mapp.

Baglio F, Blasi V, Falini A, Farina E, Mantovani F, Olivotto F, Scotti G, Nemni R, Bozzali M (2011): Functional brain changes in early parkinson's disease during motor response and motor inhibition. Neurobiol Aging 32:115–124.

Barber AD, Caffo BS, Pekar JJ, Mostofsky SH (2013): Developmental changes in within- and between-network connectivity between late childhood and adulthood. Neuropsychologia 51: 156–167.

Barnes J, Boubert L, Harris J, Lee A, David AS (2003): Reality monitoring and visual hallucinations in parkinson's disease. Neuropsychologia 41:565–574.

Berendse HW, Stam CJ (2007): Stage-dependent patterns of disturbed neural synchrony in parkinson's disease. Parkinsonism Relat Disord 13:S440–S445.

Bohnen NI, Koeppe RA, Minoshima S, Giordani B, Albin RL, Frey KA, Kuhl DE (2011): Cerebral glucose metabolic features of parkinson disease and incident dementia: Longitudinal study. J Nucl Med 52:848–855.

Bohnen NI, Minoshima S, Giordani B, Frey KA, Kuhl DE (1999): Motor correlates of occipital glucose hypometabolism in parkinson's disease without dementia. Neurology 52:541–546.

Borghammer P, Ostergaard K, Cumming P, Gjedde A, Rodell A, Hall N, Chakravarty MM (2010): A deformation-based morphometry study of patients with early-stage parkinson's disease. Eur J Neurol 17:314–320.

Braak H, Del Tredici K, Rub U, de Vos RA, Jansen Steur EN, Braak E (2003): Staging of brain pathology related to sporadic parkinson's disease. Neurobiol Aging 24:197–211.

Broyd SJ, Demanuele C, Debener S, Helps SK, James CJ, Sonuga-Barke EJ (2009): Default-mode brain dysfunction in mental disorders: A systematic review. Neurosci Biobehav Rev 33:279–296.

Burton EJ, McKeith IG, Burn DJ, Williams ED, O'Brien JT (2004): Cerebral atrophy in parkinson's disease with and without dementia: A comparison with alzheimer's disease, dementia with lewy bodies and controls. Brain 127:791–800.

Chang C, Liu Z, Chen MC, Liu X, Duyn JH (2013): EEG correlates of time-varying BOLD functional connectivity. Neuroimage 72: 227–236.

Chaudhuri KR, Schapira AH (2009): Non-motor symptoms of parkinson's disease: Dopaminergic pathophysiology and treatment. Lancet Neurol 8:464–474.

Cordes D, Haughton VM, Arfanakis K, Carew JD, Turski PA, Moritz CH, Quigley MA, Meyerand ME (2001): Frequencies contributing to functional connectivity in the cerebral cortex

in "resting-state" data. AJNR Am J Neuroradiol 22:1326–1333.

Downing PE, Chan AW, Peelen MV, Dodds CM, Kanwisher N (2006): Domain specificity in visual cortex. Cereb Cortex 16: 1453–1461.

Eberling JL, Richardson BC, Reed BR, Wolfe N, Jagust WJ (1994): Cortical glucose metabolism in parkinson's disease without dementia. Neurobiol Aging 15:329–335.

Esposito F, Tessitore A, Giordano A, De Micco R, Paccone A, Conforti R, Pignataro G, Annunziato L, Tedeschi G (2013): Rhythm-specific modulation of the sensorimotor network in drug-naive patients with parkinson's disease by levodopa. Brain 136:710–725.

Fox MD, Snyder AZ, Vincent JL, Corbetta M, Van Essen DC, Raichle ME (2005): The human brain is intrinsically organized into dynamic, anticorrelated functional networks. Proc Natl Acad Sci USA 102:9673–9678.

Fransson P (2005): Spontaneous low-frequency BOLD signal fluctuations: An fMRI investigation of the resting-state default mode of brain function hypothesis. Hum Brain Mapp 26:15–29.

Grill-Spector K (2003): The neural basis of object perception. Curr Opin Neurobiol 13:159–166.

Gusnard DA, Akbudak E, Shulman GL, Raichle ME (2001): Medial prefrontal cortex and self-referential mental activity: Relation to a default mode of brain function. Proc Natl Acad Sci USA 98:4259–4264.

Hattori T, Orimo S, Aoki S, Ito K, Abe O, Amano A, Sato R, Sakai K, Mizusawa H (2012): Cognitive status correlates with white matter alteration in parkinson's disease. Hum Brain Mapp 33: 727–739.

Helmich RC, Derikx LC, Bakker M, Scheeringa R, Bloem BR, Toni I (2010): Spatial remapping of cortico-striatal connectivity in parkinson's disease. Cereb Cortex 20:1175–1186.

Horovitz SG, Braun AR, Carr WS, Picchioni D, Balkin TJ, Fukunaga M, Duyn JH (2009): Decoupling of the brain's default mode network during deep sleep. Proc Natl Acad Sci USA 106:11376–11381.

Hu MT, Taylor-Robinson SD, Chaudhuri KR, Bell JD, Labbe C, Cunningham VJ, Koepp MJ, Hammers A, Morris RG, Turjanski N, Brooks DJ. (2000): Cortical dysfunction in non-demented parkinson's disease patients: A combined (31)P-MRS and (18)FDG-PET study. Brain 123:340–352.

Ishioka T, Hirayama K, Hosokai Y, Takeda A, Suzuki K, Nishio Y, Sawada Y, Takahashi S, Fukuda H, Itoyama Y, Mori E. (2011): Illusory misidentifications and cortical hypometabolism in parkinson's disease. Mov Disord 26:837–843.

Jubault T, Brambati SM, Degroot C, Kullmann B, Strafella AP, Lafontaine AL, Chouinard S, Monchi O (2009): Regional brain stem atrophy in idiopathic parkinson's disease detected by anatomical MRI. PLoS One 4:e8247

Jubault T, Gagnon JF, Karama S, Ptito A, Lafontaine AL, Evans AC, Monchi O (2011): Patterns of cortical thickness and surface area in early parkinson's disease. Neuroimage 55:462–467.

Karagulle Kendi AT, Lehericy S, Luciana M, Ugurbil K, Tuite P (2008): Altered diffusion in the frontal lobe in parkinson disease. AJNR Am J Neuroradiol 29:501–505.

Katzman R, Zhang MY, Ouang Ya Q, Wang ZY, Liu WT, Yu E, Wong SC, Salmon DP, Grant I (1988): A chinese version of the Mini-mental state examination; impact of illiteracy in a shanghai dementia survey. J Clin Epidemiol 41:971–978.

Klein A, Andersson J, Ardekani BA, Ashburner J, Avants B, Chiang MC, Christensen GE, Collins DL, Gee J, Hellier P, Song JH, Jenkinson M, Lepage C, Rueckert D, Thompson P, Vercauteren T, Woods RP, Mann JJ, Parsey RV. (2009): Evaluation of 14 nonlinear deformation algorithms applied to human brain MRI registration. Neuroimage 46:786–802.

Kostic VS, Agosta F, Petrovic I, Galantucci S, Spica V, Jecmenica-Lukic M, Filippi M (2010): Regional patterns of brain tissue loss associated with depression in parkinson disease. Neurology 75:857–863.

Krajcovicova L, Mikl M, Marecek R, Rektorova I (2012): The default mode network integrity in patients with parkinson's disease is levodopa equivalent dose-dependent. J Neural Transm 119:443–454.

Laatu S, Revonsuo A, Pihko L, Portin R, Rinne JO (2004): Visual object recognition deficits in early parkinson's disease. Parkinsonism Relat Disord 10:227–233.

Lowe MJ, Mock BJ, Sorenson JA (1998): Functional connectivity in single and multislice echoplanar imaging using resting-state fluctuations. Neuroimage 7:119–132.

Luo C, Song W, Chen Q, Zheng Z, Chen K, Cao B, Yang J, Li J, Huang X, Gong Q, Shang HF. (2014): Reduced functional connectivity in early-stage drug-naive parkinson's disease: A resting-state fMRI study. Neurobiol Aging 35:431–441.

Lyoo CH, Ryu YH, Lee MS (2010): Topographical distribution of cerebral cortical thinning in patients with mild parkinson's disease without dementia. Mov Disord 25:496–499.

Malach R, Reppas JB, Benson RR, Kwong KK, Jiang H, Kennedy WA, Ledden PJ, Brady TJ, Rosen BR, Tootell RB (1995): Object-related activity revealed by functional magnetic resonance imaging in human occipital cortex. Proc Natl Acad Sci USA 92:8135–8139.

Melzer TR, Watts R, MacAskill MR, Pitcher TL, Livingston L, Keenan RJ, Dalrymple-Alford JC, Anderson TJ (2012): Grey matter atrophy in cognitively impaired parkinson's disease. J Neurol Neurosurg Psychiatry 83:188–194.

Nagamachi S, Wakamatsu H, Kiyohara S, Fujita S, Futami S, Tamura S, Nakazato M, Yamashita S, Arita H, Nishii R, Kawai K. (2008): Usefulness of rCBF analysis in diagnosing parkinson's disease: Supplemental role with MIBG myocardial scintigraphy. Ann Nucl Med 22:557–564.

Nagano-Saito A, Washimi Y, Arahata Y, Kachi T, Lerch JP, Evans AC, Dagher A, Ito K (2005): Cerebral atrophy and its relation to cognitive impairment in parkinson disease. Neurology 64: 224–229.

Nishio Y, Hirayama K, Takeda A, Hosokai Y, Ishioka T, Suzuki K, Itoyama Y, Takahashi S, Mori E (2010): Corticolimbic gray matter loss in parkinson's disease without dementia. Eur J Neurol 17:1090–1097.

Olde Dubbelink KT, Schoonheim MM, Deijen JB, Twisk JW, Barkhof F, Berendse HW (2014): Functional connectivity and cognitive decline over 3 years in parkinson disease. Neurology 83:2046–2053.

Peppard RF, Martin WR, Carr GD, Grochowski E, Schulzer M, Guttman M, McGeer PL, Phillips AG, Tsui JK, Calne DB (1992): Cerebral glucose metabolism in parkinson's disease with and without dementia. Arch Neurol 49:1262–1268.

Pieri V, Diederich NJ, Raman R, Goetz CG (2000): Decreased color discrimination and contrast sensitivity in parkinson's disease. J Neurol Sci 172:7–11.

Price MJ, Feldman RG, Adelberg D, Kayne H (1992): Abnormalities in color vision and contrast sensitivity in parkinson's disease. Neurology 42:887–890.

Raichle ME, MacLeod AM, Snyder AZ, Powers WJ, Gusnard DA, Shulman GL (2001): A default mode of brain function. Proc Natl Acad Sci USA 98:676–682.

Rektorova I, Krajcovicova L, Marecek R, Mikl M (2012): Default mode network and extrastriate visual resting state network in patients with parkinson's disease dementia. Neurodegener Dis 10:232–237.

Samann PG, Wehrle R, Hoehn D, Spoormaker VI, Peters H, Tully C, Holsboer F, Czisch M (2011): Development of the brain's default mode network from wakefulness to slow wave sleep. Cereb Cortex 21:2082–2093.

Schnitzler A, Gross J (2005): Normal and pathological oscillatory communication in the brain. Nat Rev Neurosci 6:285–296.

Schwartzman RJ, Alexander GM, Ferraro TN, Grothusen JR, Stahl SM (1988): Cerebral metabolism of parkinsonian primates 21 days after MPTP. Exp Neurol 102:307–313.

Tessitore A, Esposito F, Vitale C, Santangelo G, Amboni M, Russo A, Corbo D, Cirillo G, Barone P, Tedeschi G (2012): Default-mode network connectivity in cognitively unimpaired patients with parkinson disease. Neurology 79:2226–2232.

Uc EY, Rizzo M, Anderson SW, Qian S, Rodnitzky RL, Dawson JD (2005): Visual dysfunction in parkinson disease without dementia. Neurology 65:1907–1913.

Vanhaudenhuyse A, Demertzi A, Schabus M, Noirhomme Q, Bredart S, Boly M, Phillips C, Soddu A, Luxen A, Moonen G, Laureys S. (2011): Two distinct neuronal networks mediate the awareness of environment and of self. J Cogn Neurosci 23:570–578.

Weintraub D, Doshi J, Koka D, Davatzikos C, Siderowf AD, Duda JE, Wolk DA, Moberg PJ, Xie SX, Clark CM (2011): Neurodegeneration across stages of cognitive decline in parkinson disease. Arch Neurol 68:1562–1568.

Zalesky A, Fornito A, Bullmore ET (2010): Network-based statistic: Identifying differences in brain networks. Neuroimage 53: 1197–1207.

Zarei M, Ibarretxe-Bilbao N, Compta Y, Hough M, Junque C, Bargallo N, Tolosa E, Marti MJ (2013): Cortical thinning is associated with disease stages and dementia in parkinson's disease. J Neurol Neurosurg Psychiatry 84:875–881.

Zhang J, Wei L, Hu X, Zhang Y, Zhou D, Li C, Wang X, Feng H, Yin X, Xie B, Wang J. (2013): Specific frequency band of amplitude low-frequency fl uctuation predicts parkinson's disease. Behav Brain Res 252:18–23.

Zhang MY, Katzman R, Salmon D, Jin H, Cai GJ, Wang ZY, Qu GY, Grant I, Yu E, Levy P, Klauber MR, Liu WT. (1990): The prevalence of dementia and alzheimer's disease in shanghai, china: Impact of age, gender, and education. Ann Neurol 27: 428–437.